

Proceeding to the LHC seminar talk *Update of the  $B^0 \rightarrow K^{*0} \mu^+ \mu^-$  angular analysis at LHCb* held by Eluned Smith on behalf of the LHC collaboration on 13th of March 2020.

Nils Breer

Technische Universität Dortmund

The stated Process is of such importance because the  $b \rightarrow s\mu\mu$  transition is forbidden at tree level due to FCNC. A study of this is preferably done with indirect searches because the energy scales can be set much larger than in direct searches, therefore new Physics(NP) is more accessible.

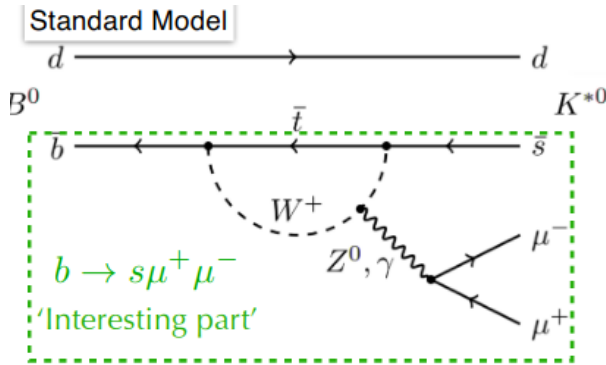


Figure 1: Process in standard model.

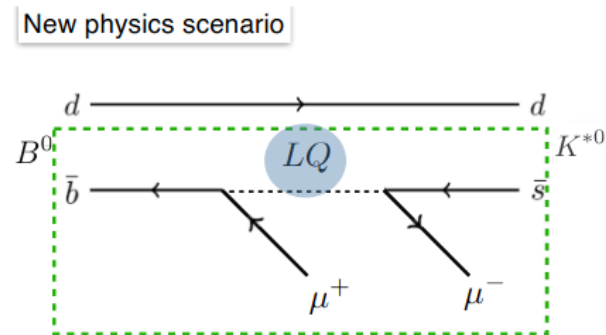


Figure 2: Process in new physics model.

In figure 2[1], instead of a suppressed loop via a W-boson which decays weak into a neutral gauge boson and then further into two muons, the NP model suggest a leptoquark as "gauge

boson". Leptoquarks (mostly denoted as X- and Y-Boson) are particles postulate by the GIM model, which provides a way to change a quark into a lepton via the decay channel

$$X \rightarrow l^+ + \bar{D}$$

## 1 transition in effective theory

Instead of calculating the well known transition via box diagram, we now factorize out the loops and replace them with an effective coupling (analogous to 4f coupling). This results in a 4-particle-vertex which is now described with Wilson coefficients which are sensitive to NP.

With these changes an effective Hamiltonian  $H_{eff}$  can be written as

$$H_{eff} = -\frac{4G_f}{\sqrt{2}} V_{tb} V_{ts}^* \sum_i (C_i \cdot O_i + C_i' \cdot O_i')$$

where  $C_i$  are the short ranged Wilson coefficients which we want to study. The  $O_i$  are the long distance, low energy QCD operators which follow the formfactors.

## 2 angular Analysis

With the angular analysis we want to measure the decay rate of a process as a function of the final state decay angles, which are schematically shown in figure 3.

The three important angles are  $\theta_k$ ,  $\theta_l$  and  $\phi$ . Because the two leptons and the Kaon and Pion are produced in sort of opposite directions,  $\theta_k$  is the angle between the Kaon and the vector sum of the Kaon and the Pion, which is the

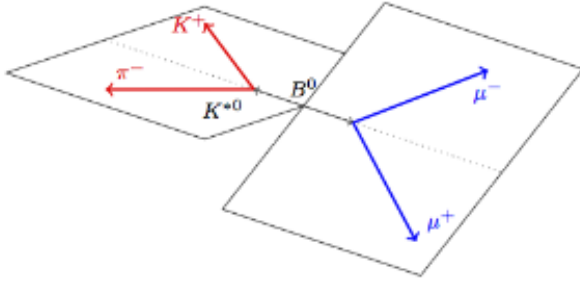


**Figure 3:** schematical image of decay angles.

general flight direction. For  $\theta_l$  it is the same argumentation but for the positive lepton and the flight direction of the leptons.

In general, the leptons do not fly in the exact same direction, so their direction vector span a plane. This is also true for the Pion and the Kaon. The angle  $\phi$  is the angle between the normal vector of the K- $\pi$ -plane and the  $\mu$ - $\mu$ -plane. This analysis can give access to more observables with reduced uncertainties.

### 3 early LHCb Measurements and local tension

Angular analysis for local tension in  $P'_5$  performed by other collaborations such as ATLAS and CMS show similar results but Data taken stops at roughly the  $J\Psi$  Mass due to the resonant background. Therefore the ATLAS measurement is not so good. As seen in some global fits, the shift in the wilson coefficient  $\text{Re}(C_9)$ , the deviations in these wilson coefficients or up to 3 - 5  $\sigma$ . In general, these fits are a good tool to learn from the fits.

### 4 the data set and Selection of Candidates

The data used comes from the years 2011, 2012, which was Run 1, and 2016. The center of mass energies were 7, 8 and 13 TeV respectively. The data taken in the later years is nearly double from what they have taken in 2011.

For the stated process, it is required that the impact parameter for the daughters are quite large because they don't come from the primary

vertex. Also the PID<sup>1</sup> is used to suppress the peaks in the background. Machine learning algorithms are used to reduce combinatorial background. For the probe regions in the  $q^2$  plot, the signal regions must be separated from the background regions. Since there are decay modes which have the same final state as our wanted process, there are several peak regions which must be cut out. This is for example the charmonium background of the  $J\Psi$  and the  $\psi$  meson. The signal regions for the decay mode  $b \rightarrow s\mu\mu$  can be interpreted separately. Also the photon pole at  $q^2 = 0$  can be examined. The binning used is historically conditioned. The only cause for that is to compact the data. One boundary at 1.1 GeV is set to delete the  $\phi(1020)$  resonance from the data.

### 5 angular fit model

To describe now the physics behind the angular analysis, instead of using the non-perturbative QCD form factors and the wilson coefficients, angular amplitudes  $A^{LR}$  are defined. Then we measure in the bins of  $q^2 = m^2(\mu\mu)$  by firstly integrating over  $q^2$  and secondly combining this with the  $B^0$  and  $\bar{B}^0$  decays. This results in a so called CP-averaged basis  $S_i$ . The resulting  $\frac{d\Gamma}{dq^2}$  spectrum is then

$$\frac{1}{\frac{d(\Gamma+\bar{\Gamma})}{dq^2}} \cdot \frac{d(\Gamma+\bar{\Gamma})}{d\cos\theta_l d\cos\theta_k d\phi} \Big|_P = \frac{9}{32\pi} \cdot f(F_L, \theta_k, \theta_l, A_{FB}, S_i)$$

Here, the  $F_L$  describes the fraction of longitudinal polarisation of the  $K^{0*}$ .  $A_{FB}$  is the forward/backward asymmetry of the dimuon system. In order to reduce uncertainties, the first basis of the  $S_i$  is transformed into a basis  $P_i$  which takes ratios of observables[1].

### 6 full fit model

In the full fit model the shape of the invariant mass plots are used to determine the amount of signal and background in the data.

$$\text{PDF}_{total} = f_{sig} \text{PDF}_{sig}(\vec{\Omega}, m) + (1-f_{sig}) \text{PDF}_{bkg}$$

<sup>1</sup>particle identification

The PDF function can be separated into an angular part and a massive part. After that a maximum likelihood fit is performed. As seen in figure 4 the massive part of the signal PDF is a gaussian function with a radiative tail and the background PDF results in a exponential function.

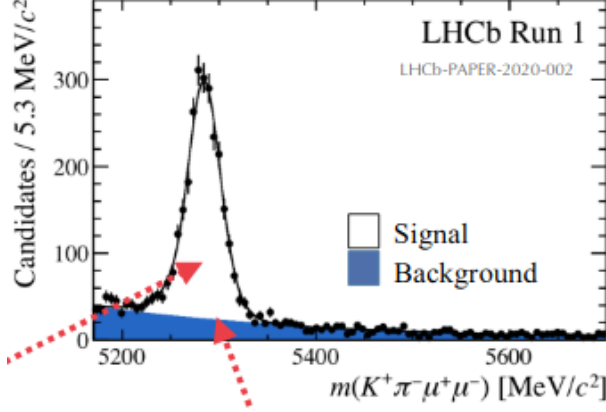


**Figure 4:** invariant B mass of Run 1 LHCb data.

Because of the factorization of the signal and background PDF

$$\text{PDF}_{sig}(\vec{\Omega}, m) = \text{PDF}_{sig}(\vec{\Omega}) \times \text{PDF}_{sig}(m)$$

the angular part of the signal PDF of the Run 1 data and the data from 2016 can be shared in the analysis to perform a simultaneous fit  $\sum_I S_{i,q_{bin}^2} f_i(\Omega)$ .

## 7 modelling the efficiencies

Because the angular distribution and the  $q^2$  distribution are influenced by the efficiencies, the parametrisation must be well known. This is done via an acceptance function, here the legendre polynomials. With 3 angles and  $q^2$  a 4D parametrisation results in 4 coefficients

## 8 s-wave contribution

The  $K\pi$  final state has more than one spin eigenstate. Therefore, additional terms are needed to differentiate between these states. Because  $K\pi\mu\mu$  can be produced in a vector state which disturbs the angular distribution, the different structures of the spin 1  $K^{0*}$  and the flat structure of the  $K\pi$  state need to be analyzed.

## 9 uncertainties

The dominant systematic uncertainties across the  $q^2$  bins are acceptance variation with  $q^2$ , peaking backgrounds and the bias correction. The whole table of uncertainties is shown in figure 5[1].

Source	$F_L$	$S_3-S_9$	$P_1-P'_8$
Acceptance stat. uncertainty	< 0.01	< 0.01	< 0.01
Acceptance polynomial order	< 0.01	< 0.01	< 0.02
Data-simulation differences	< 0.01	< 0.01	< 0.01
Acceptance variation with $q^2$	< 0.03	< 0.01	< 0.09
$m(K^+\pi^-)$ model	< 0.01	< 0.01	< 0.01
Background model	< 0.01	< 0.01	< 0.02
Peaking backgrounds	< 0.01	< 0.02	< 0.03
$m(K^+\pi^-\mu^+\mu^-)$ model	< 0.01	< 0.01	< 0.01
$K^+\mu^+\mu^-$ veto	< 0.01	< 0.01	< 0.01
Trigger	< 0.01	< 0.01	< 0.01
Bias correction	< 0.02	< 0.01	< 0.03

**Dominant systematics in each observable category**

**Figure 5:** table of systematic uncertainties.

Because of different decays in the same target finalstate, for example  $\bar{A}_b^0 \rightarrow \bar{p} \rightarrow \pi^- K^+ \mu\mu$ , events that are drawn from distributions of these peaking backgrounds are not taken into the fit. Bias corrections come up if boundary effects like  $F_S > 0$  are required.

$$\frac{d\Gamma}{dq^2}|_{S+P} = (1 - F_S) \frac{d\Gamma}{dq^2}|_P$$

For small  $F_S$  the bias towards higher values biases the P-wave and vice versa.

## 10 Results and conclusion

If the energy threshold is so big, that a  $c\bar{c}$  pair can be produced in a loop which generates a  $J\psi$ , the would be a possibility to detect it. The tension is confirmed with the 2016 data set. The significance of the discrepancy is nuisance parameter dependend and also depends on the  $q^2$  bins.

## References

- [1] Elune Anne Smith. *Updated angular analysis of the decay  $B^0 \rightarrow K^{*0}(\rightarrow K^+\pi^-)\mu^+\mu^-$* . URL: <https://indi.to/bMm9K> (visited on 07/17/2020).